[23] J. R. Mosig and F. E. Gardiol, "Analytical and numerical techniques in the Green's function treatment of microstrip antennas and scatterers," *IEE Proc., Part H—Microw., Opt. Antennas*, vol. 130, no. 2, pp. 175–182, 1983.
[24] J. R. Mosig, "Integral equation techniques," in *Numerical Techniques for Microwave and Milimeter-Wave Passive Structures*, T. Itoh, Ed. New York: Wiley, 1989, pp. 133–213.
[25] H. H. H. Homeier, "Scalar Levin-type sequence transformations," *J. Comput. Appl. Math.*, vol. 122, no. 1–2, pp. 81–147, 2000.
[26] T. Ooura and M. Mori, "A robust double exponential formula for Fourier-type integrals," *J. Comput. Appl. Math.*, vol. 112, no. 1–2, pp. 229–241, 1999.
[27] T. N. L. Patterson, "Algorithm 468: Algorithm for automatic numerical integration over a finite interval," *Commun. ACM*, vol. 16, no. 11, pp. 694–699, 1973.

Diversity On-Glass Antennas for Maximized Channel Capacity for FM Radio Reception in Vehicles

Seungbeom Ahn, Yong Soo Cho, and Hosung Choo

***Abstract*—This communication proposes a systematic design method to increase the diversity gain for vehicle on-glass antennas using the Pareto genetic algorithm. The initial antenna structure consists of two FM antennas printed on a rear window with horizontal conducting striplines. The position and the number of the vertical lines in the rear window were then determined using the Pareto genetic algorithm to maximize the channel capacity and average bore-sight gain of each antenna. The optimized antennas were built and mounted in a commercial sedan, and the antennas' performances, such as the reflection coefficient, radiation pattern, and channel capacity were measured. The measurements showed a matching bandwidth of around 15% and an average bore-sight gain of more than -12 dBi. The measured correlation coefficient of the two antennas was less than 0.6.**

***Index Terms*—Channel capacity, correlation coefficient, diversity on-glass antennas.**

I. Introduction

FM radio is one of the most popular communication systems utilized in current vehicle design [1]. Customers expect a high quality reception from their FM radios, although they drive their vehicles in various environments. Thus, most of the vehicle manufacturers put considerable effort into improving their radio systems and compete to offer their own performance standard in FM reception. An FM radio consists of a tuner, an amplifier, a connection cable, and a receiving antenna. Of these, the receiving antenna is probably the most important unit because of its critical effect on the reception performance.

Manuscript received February 12, 2010; revised June 10, 2010; accepted October 26, 2010. Date of publication December 03, 2010; date of current version February 02, 2011. This work was supported by the Hyundai Kia Motors and the IT R&D program of MKE/KEIT [KI002084, A Study on Mobile Communication System for Next-Generation Vehicle with Internal Antenna Array].

S. Ahn is with the RFID Team, Convergence R&D Center, LS Industrial Systems, Anyang 431-749, Korea (e-mail: sbahn@lsis.biz).
Y. S. Cho is with the School of Electronics and Electrical Engineering, Chung-Ang University, Seoul 156-756, Korea (e-mail: yscho@cau.ac.kr).
H. Choo is with the School of Electronic and Electrical Engineering, Hongik University, Seoul 121-791, Korea (e-mail: hschoo@hongik.ac.kr).

Color versions of one or more of the figures in this communication are available online at http://ieeexplore.ieee.org.
Digital Object Identifier 10.1109/TAP.2010.2096188

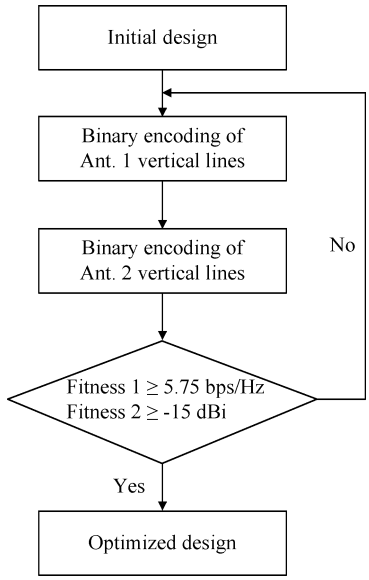

Fig. 1. Block diagram of the PGA design procedure.

Monopole type antennas, such as tuned-monopoles, micro-antennas, and shark fin antennas, have been widely used in numerous vehicle designs [2], [3]. These antennas, however, suffer from a lack of durability, high aerodynamic resistance, and an undesirable appearance, as they protrude from the vehicle's exterior. To mitigate these problems, on-glass antennas have been developed and are now commonly applied in modern vehicle designs. On-glass antennas also have the advantage of having a low manufacturing cost, due to the antennas being printed directly onto the vehicle window [4], [5]. However, they usually suffer from narrow matching bandwidth, low antenna gain, and radiation nulls, because the stripline of an on-glass antenna is printed onto the glass with a high dielectric loss. Also, the on-glass antennas show performance deterioration in urban environments where the channel characteristics are predominated by multi-path fading [6]. Recently, to improve the receiving performance, some luxury vehicles have employed diversity on-glass antennas systems that incorporate two separate antennas in a single window.

In this communication, we propose a systematic design method for diversity on-glass antennas that make them suitable for FM radio reception in a commercial sedan. The basic structure of the diversity on-glass antenna incorporates two FM antennas placed on the upper and lower areas of the rear window [7]–[9]. The horizontal lines of the antennas are commonly used as defroster lines, so the position and the number of the vertical lines were determined using the Pareto genetic algorithm (PGA) to maximize the channel capacity and average bore-sight gain of each antenna. The optimized on-glass antennas were built and mounted on a commercial sedan, and the antenna performance, such as the reflection coefficient and the bore-sight gain, were measured in a semi-anechoic chamber. The measurement showed a half-power bandwidth of around 15% and a bore-sight gain of over -20 dBi in the FM radio band. To confirm the diversity performance in a real situation, we measured the received FM signal power in an urban environment, where multi-path fading exists, which revealed low correlation coefficients of 0.52 between the diversity on-glass antennas.

II. Antenna Structure and Optimization

Fig. 1 shows a block diagram of the proposed design method for diversity on-glass antennas. The detailed designs of the antennas were

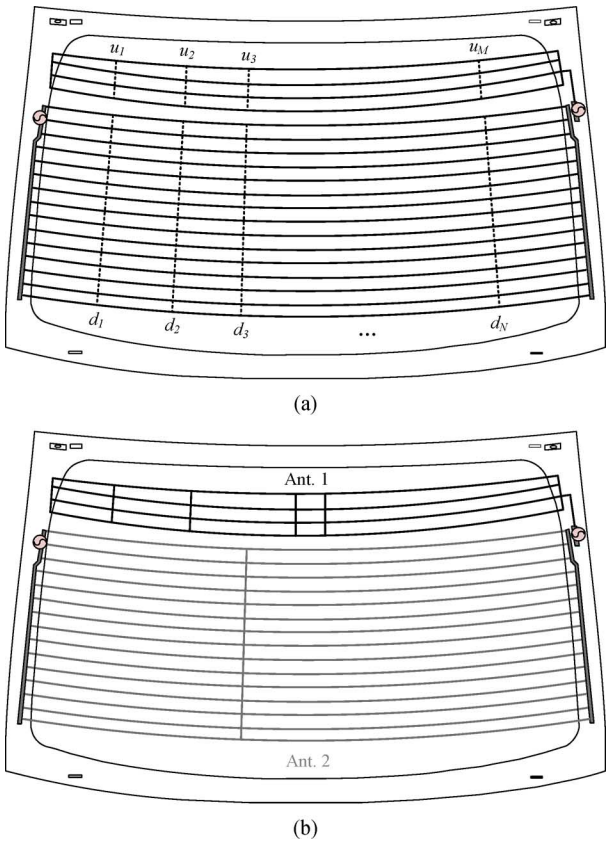

Fig. 2. Antenna geometry: (a) Design parameters. (b) Optimized design.

determined using PGA to maximize the channel capacity and average bore-sight gain of each antenna [10]. Fig. 2(a) shows the basic antenna structure, and it consists of horizontal conducting striplines ($\sigma = 5.7 \times 10^7$) printed on the glass ($\varepsilon_r = 7$, $\tan\delta = 0.03$ at 100 MHz) in the upper and lower areas of the rear window. The horizontal lines of on-glass antennas are also used as defroster lines, so the length (L_h), interval distance (i_h), and number (N_h) of the horizontal lines are strictly restricted. They were given as $L_h = 120$ cm, $i_h = 3$ cm and $N_h = 19$ (Ant. 1: 4, Ant. 2: 15) for a commercial sedan (2007 Hyundai Grandeur TG Q 240). We then optimized the number and the position of the vertical lines in order to increase the channel capacity and raise the radiation gain of the diversity antennas.

In the PGA process, the upper antenna (Ant. 1) of 1,110 mm × 79 mm can have M number of conducting vertical lines ($u_1, u_2, \ldots, u_M$), and the lower antenna (Ant. 2) of 1,200 mm × 418 mm can have N number of conducting vertical lines ($d_1, d_2, \ldots, d_N$). The shape of the vertical lines were then encoded as a binary chromosome of $M+N$ bits where "1" bit means a vertical line exits and "0" bit means a vertical line is deleted. The two antennas were extended to the window frames of the vehicle by connection lines (15 cm), and they were fed by 50 Ω coaxial cables

$$fitness\,1 = \frac{1}{N_F}\left\{\sum_{i=1}^{N_F} C\left(f_i\right)\right\} \tag{1}$$

$$fitness\,2 = \frac{1}{2\cdot N_F} \cdot \sum_{j=1}^{2}\sum_{i=1}^{N_F}[Gain_{Ant.j}\left\{f_i\,;(\theta = 90^\circ, \phi = 180^\circ)\right\}]. \tag{2}$$

The final design goals in this process were to achieve a high channel capacity and good radiation characteristics. To improve the channel capacity of the on-glass antenna, we included the channel capacity fitness function as shown in (1), where C is the channel capacity of antennas and f_i is frequency from 70 MHz to 130 MHz ($N_F = 13$). To increase the average gain of the antennas, we included the second fitness function as shown in (2), which represents the average gain of two antennas ($j = 1$ is Ant. 1 and $j = 2$ is Ant. 2) along the bore-sight direction ($\theta = 90$, $\phi = 180^\circ$). The 3-D radiation patterns from the EM simulation were used to obtain the channel capacity which is an important performance criterion for diversity systems. To obtain the channel capacity, the correlation coefficient was calculated, as follows:

$$\psi_{ij} = \frac{1}{\sigma_i \sigma_j}\oint E\left[\left\{\mathbf{A_i}\left(\Omega\right)\cdot\mathbf{E}\left(\Omega\right)\right\}\ \left\{\mathbf{A_j^*}\left(\Omega\right)\cdot\mathbf{E}^*\left(\Omega\right)\right\}\right] d\Omega \tag{3}$$

where $\mathbf{A}_i\left(\Omega\right)$, $\mathbf{A}_j\left(\Omega\right)$ are 3-D radiation patterns of the individual antennas i and j, $\mathbf{E}\left(\Omega\right)$ is a random incident field. σ is the variance of multiplication between the $\mathbf{A}\left(\Omega\right)$ and $\mathbf{E}\left(\Omega\right)$, and Ω is the solid angle over (θ, ϕ) [11]. To consider the vehicle mobility, the elevation angle of the incident field has a Gaussian distribution with a mean of $\theta = 90^\circ$ and a variance of 30°. The azimuth angle of the incident field has a uniform distribution. Based on the correlation coefficient between the two antennas, we calculated the ergodic channel capacity using the following:

$$C = E\left[\log_2\left\{\det\left(I_{n_R} + \frac{\rho}{n_T}\widetilde{\mathbf{H}}\boldsymbol{\Psi}\widetilde{\mathbf{H}}^*\right)\right\}\right] \tag{4}$$

where n_T, n_R are numbers of the transmitting and receiving antennas, $\tilde{\mathbf{H}}$ is an normalized transfer matrix, and ρ is a signal-to-noise ratio. The Rayleigh fading channel model, which represents the multi-path fading environment, was used for the transfer matrix [11]. To accurately estimate the antenna performance, such as a 3-D radiation pattern and bore-sight gain, we used a full-wave EM simulator (FEKO of *EM software and systems*) [12]. In our EM simulation, the striplines printed on the window were modeled as a coated wire for faster and accurate simulation [13]. Also, an entire vehicle body of the commercial sedan was included in our simulation as approximately 4,200 piece-wise triangular meshes.

Fig. 2(b) shows the optimized antenna using the proposed design procedure shown in Fig. 1, and it shows four vertical lines for Ant. 1 and a single vertical line for Ant. 2. The channel capacity for the optimized antenna was 5.77 bps/Hz, while the theoretical maximum value of the channel capacity is 5.8 bps/Hz ($n_T = n_R = 2$, $\rho = -10$ dB). The average bore-sight gain for Ant. 1 was -9.25 dBi and for Ant. 2 was -14.72 dBi. To verify the performance of the optimized antennas, antennas were built on the rear window of a commercial sedan, and antenna characteristics were measured in a semi-anechoic chamber as well as in actual outdoor conditions [14].

III. Measurement and Analysis

The measurement was performed using an Agilent E5071A network analyzer with an ETS-Lindgren 3121C dipole as the transmitter in a semi-anechoic chamber of 30 m × 30 m. Fig. 3 shows the measured reflection coefficient of the proposed antennas. The solid line represents the reflection coefficient of Ant. 1, and the dashed line represents that of Ant. 2. The result shows matching bandwidth ($\Gamma_{\rm dB} < -3$ dB) of 17.5% for Ant. 1 and 21.5% for Ant. 2. Ant. 1 has a better impedance matching at higher frequency (112.5 MHz ~ 130 MHz), and Ant. 2 has a better impedance matching at lower frequency (73.5 MHz ~ 95 MHz). Fig. 4 shows the measured bore-sight gain of Ant. 1 (solid line) and Ant. 2 (dashed line). The proposed antennas showed bore-sight vertical gain of more than -20 dBi in the FM radio band. The average

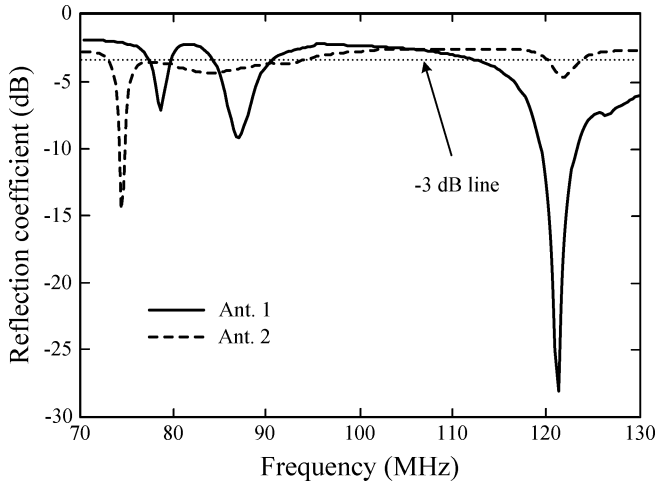

Fig. 3. Measured reflection coefficient of Ant. 1 (———) and Ant. 2 (- - - - -).

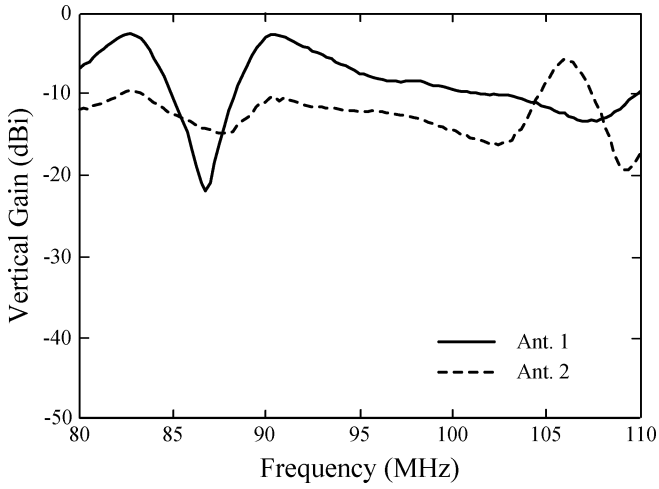

Fig. 4. Measured bore-sight gain of Ant. 1 (———) and Ant. 2 (- - - - -).

bore-sight vertical gains of the two antennas were also -7.58 dBi and -11.57 dBi, and they were higher than -12 dBi which was the requested specifications from a particular motor company. The vertical gain of Ant. 1 was higher than Ant. 2, while the horizontal gain of Ant. 2 was higher than Ant. 1. Thus, the total gain of Ant. 1 was about the same as Ant. 2. Fig. 5 shows the comparison between the simulated and measured vertical radiation patterns of the two antennas in azimuth direction ($\theta = 90^{\circ}$) at 100 MHz. Fig. 5(a) illustrates radiation patterns of Ant. 1, and Fig. 5(b) illustrates radiation patterns of Ant. 2. The measured radiation patterns (solid line) agree well with the simulated radiation patterns (dashed line). To explore the effect of passengers in the back seat on the antenna performance, we added the cylindrical dielectric body (similar dielectric constant to a human body: $\varepsilon_{\mathrm{r}} = 75$ and $\sigma = 0.95\ \mathrm{S/m}$) in the simulation. The impedance and bandwidth were similar to that without the cylindrical body, and the vertical gains of Ant. 1 and Ant. 2 were slightly decreased from -7.58 dBi to -8.41 dBi and from -11.57 dBi to -12.00 dBi, respectively. To examine the diversity characteristics of the proposed antenna depending on the design geometry, we calculated channel capacity when varying the number of the two antennas' vertical lines. Fig. 6 shows the channel capacity with M and N representing the number of vertical lines in Ant. 1 and Ant. 2, respectively. The maximum channel capacity of 5.77 bps/Hz was observed when the antennas have $\mathrm{M} = 4, \mathrm{N} = 1$. Also,

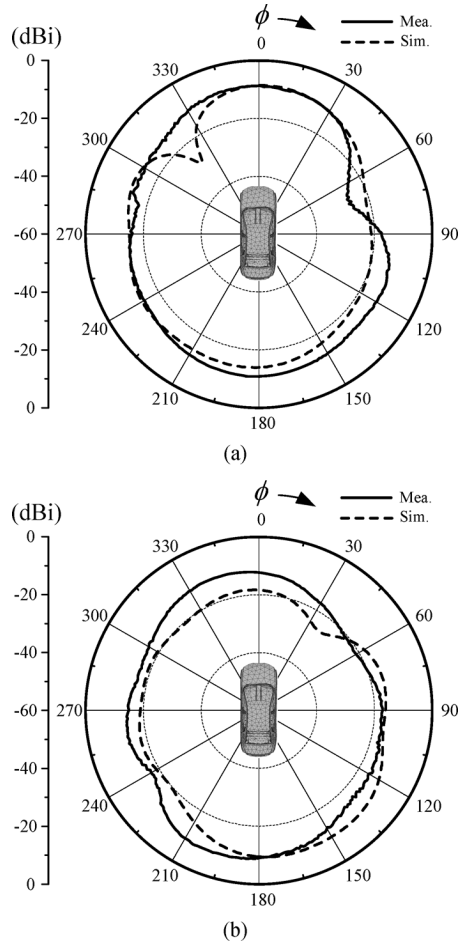

Fig. 5. Measured (———) and simulated (- - - - -) radiation patterns of antennas: (a) Ant. 1. (b) Ant. 2.

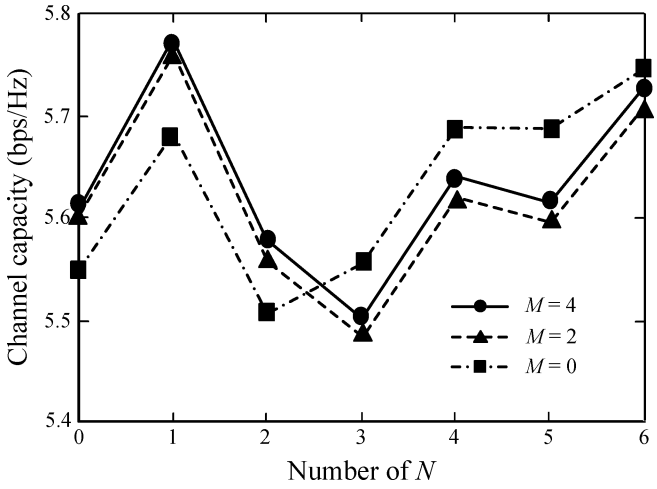

Fig. 6. Channel capacity by the number of vertical lines (N) of Ant. 2 when vertical lines of Ant. 1 are $M = 4$ (—•—), $M = 2$ (– –▲– –), and $M = 0$ (-·- ■-·-).

the BER was calculated in terms of the SNR using the correlation coefficient based on the selection combining system, which consists of a transmitting antenna and two receiving antennas. For the SNR of 10 dB, the non-diversity antenna has the BER of 3.4×10^{-3}. Based on the BER, the optimized diversity antennas ($\mathrm{M} = 4, \mathrm{N} = 1$) shows

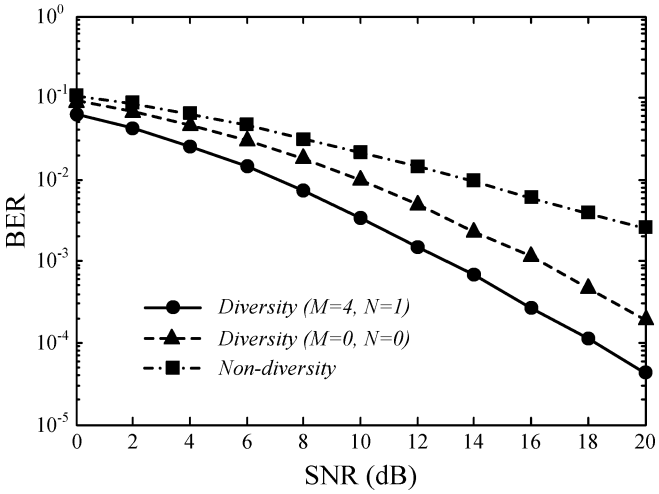

Fig. 7. BER vs. SNR in SC system when vertical lines of Ant. 1 and Ant. 2 are $M = 4$, $N = 1$ (—•—), $M = 0$, $N = 0$ (– –▲– –), and Non-diversity (-·-■-·-).

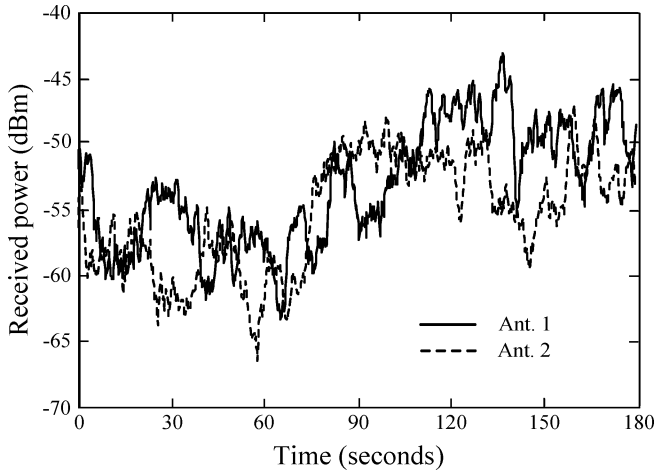

Fig. 8. Received power level in terms of time for Ant. 1 (———) and Ant. 2 (- - - - -).

the SNR of 4.53 dB, and thus the diversity gain is 5.47 dB, which is close to an ideal diversity gain of 5.9 dB.

To confirm the diversity performance in a real situation, we measured the received FM signal strength in actual outdoor conditions where the channel characteristics are predominated by the multi-path fading of an urban environment (Yeouido, Seoul, Korea). When driving the sedan, we measured the transmitting signal of the Kyonggi broadcast that transmits the signal power of 5 kW with 99.9 MHz from Gwanggyo base station (The distance from Gwanggyo to Yeouido is about 30 km.). The vehicle speed was about 20 km/h and the travelled distance was 1.2 km (driving time: 180 seconds). In the measurement, we sampled the received power 3 times per second in real time using a laptop computer connected to an Agilent 8593 A spectrum analyzer by a USB-GPIB controller. Fig. 8 shows the received powers of Ant. 1 (solid line) and Ant. 2 (dashed line). The received power levels of the two antennas were very different, and they varied rapidly according to time of measurement. Ant. 1 showed the average received power of -53.09 dBm which is 2 dB higher than that of Ant. 2. The correlation coefficient between the received signal powers of the two antennas was calculated as shown in Table I. The correlation coefficients, averaged for each 30 seconds duration were ranging from 0.18 to 0.62, and the averaged for the total 180 seconds was 0.52. Thus, if the selection combining, which is to choose the antenna signal with the higher power level, is used for this measurement condition, the average power of 52.05 dBm can be observed (1 dB higher than the average power of Ant. 1).

TABLE I
CORRELATION COEFFICIENT BETWEEN THE RECEIVED SIGNAL POWERS

Time(s)	0-30	30-60	60-90	90-120	120-150	150-180	Total
Correlation coefficient	0.18	0.52	0.62	0.44	0.27	0.19	0.52

IV. CONCLUSION

This communication proposed the design of diversity on-glass antennas with a high channel capacity and good radiation characteristics. We optimized the position and number of vertical lines in the rear window of a vehicle using the PGA procedure. The proposed diversity antennas were built into the rear window of a vehicle, and performances were measured. The measurements showed a matching bandwidth of around 15% and an average bore-sight gain of more than -12 dBi. The measured correlation coefficient using the FM broadcasting signal strength of the two antennas was less than 0.6. These results verify that the proposed diversity antennas are suitable for FM radio reception in vehicles.

REFERENCES

[1] S. Egashira, T. Tanaka, and A. Sakitani, "A design of AM/FM mobile telephone triband antenna," *IEEE Trans. Antennas Propag.*, vol. 42, no. 4, pp. 538–540, Apr. 1994.

[2] K. Yegin, "On-vehicle GPS antenna measurements," *IEEE Antennas Wireless Propag. Lett.*, vol. 6, pp. 488–491, Jun. 2007.

[3] L. Low, R. J. Langley, R. Breden, and P. Callaghan, "Hidden automotive antenna performance and simulation," *IEEE Trans. Antennas Propag.*, vol. 54, no. 12, pp. 3707–3712, Dec. 2006.

[4] Y. Noh, Y. Kim, and H. Ling, "Broadband on-glass antenna with meshgrid structure for automobiles," *Electron. Lett.*, vol. 41, no. 21, pp. 1148–1149, Oct. 2005.

[5] J. C. Batchelor, R. J. Langley, and H. Endo, "On-glass mobile antenna performance modeling," *IEE Proc.-Microw. Antennas Propag.*, vol. 148, no. 4, pp. 233–238, Aug. 2001.

[6] R. G. Vaughan and J. B. Andersen, "Antenna diversity in mobile communications," *IEEE Trans. Veh. Tech.*, vol. 36, no. 4, pp. 149–172, Nov. 1987.

[7] Y. Kim and E. K. Walton, "Automobile conformal antenna design using non-dominated sorting genetic algorithm," *IEE Proc.-Microw. Antennas Propag.*, vol. 153, no. 6, pp. 579–582, Dec. 2006.

[8] M. Ohnishi, Y. Nagayama, and S. Tadokoro, "Automotive Window Glass Antenna," U.S. patent no. 5461391, Oct. 1995.

[9] L. Heinz, H. Jochen, R. Leopold, and F. Gerhard, "Mehrantennenanordnung für Antennendiversity in Einer Fensterscheibe," E.P. Patent no. 0297328, Jan. 1989.

[10] J. Horn, N. Nafpliotis, and D. E. Goldberg, "A niched Pareto genetic algorithm for multiobjective optimization," in *Proc. IEEE Evolutionary Computation Conf.*, 1994, vol. 1, pp. 82–87.

[11] L. Dong, H. Choo, R. W. Heath, and H. Ling, "Simulation of MIMO channel capacity with antenna polarization diversity," *IEEE Trans. Wireless Commun.*, vol. 4, no. 4, pp. 1869–1873, Jul. 2005.

[12] FEKO Comprehensive EM Solutions [Online]. Available: http://www.feko.info/

[13] R. W. P. King, "Wire and strip conductors over a dielectric-coated conducting or dielectric half-space," *IEEE Trans. Microw. Theory Tech.*, vol. 37, no. 4, pp. 754–760, Apr. 1989.

[14] Hyundai Grandeur TG Q 240 2007 [Online]. Available: http://www.hyundai.com